DAMAGE AND FAILURE OF BRITTLE SOLIDS

Andrzej Litewka[*], Leszek Szojda[**]
[*]*Universidade da Beira Interior, Calçada Fonte do Lameiro, P 6200-358 Covilhã, Portugal*
[**]*Silesian University of Technology, Akademicka 5, PL 44-100 Gliwice, Poland*

Summary The aim of this paper is to study the process of the damage growth that results in material failure for rock-like cementitious brittle materials subjected to multi-axial state of stress. To this end the stress-strain curves and stress at failure were determined experimentally for cylindrical specimens of mortar under tri-axial state of stress. These experimental results were compared with the theoretical predictions obtained from the own theoretical model based on the methods of the damage mechanics.

INTRODUCTION

To formulate more precise theoretical models capable to describe the physical processes observed in materials subjected to complex loading the deeper theoretical and experimental studies of mechanical properties of materials are required. The results of such analyses available in the literature show that deformation of brittle rock-like materials and cementitious composites is accompanied by development of oriented cracks and that an amount and configuration of this internal damage are closely connected with the magnitude and directions of the principal stresses applied. That is why, some theoretical models based on the methods of the damage mechanics were formulated to describe the mechanical behaviour of concrete and rocks [1,2,3,4]. However, the realistic theoretical description of overall material response accounting for oriented damage growth and for development of damage induced anisotropy of such materials the extensive experimental studies are needed. The aim of this note is to supply new experimental data for brittle material subjected to tri-axial state of stress as well as presentation of the theoretical model capable to describe deformability and failure of initially isotropic brittle rock-like solids.

EXPERIMENTS

The experimental results presented in this note were obtained for 16 cylindrical specimens of mortar subjected to tri-axial compression. The tests were performed in testing machine ZD40 of 400 kN capacity combined with the hydraulic attachment necessary to apply a lateral compression. Longitudinal and lateral deformations of the specimen were measured by means of four electrical resistance strain gauges arranged in the form of two cruciform rosettes glued on the opposite sides of the cylinders. The programme of loading consisted of uni-axial compression (four specimens) and two cases of tri-axial loading referred to as tri-axial state of stress 1 (six specimens) and tri-axial state of stress 2 (six

Table 1. Experimental data and constants used in analysis of tri-axial state of stress of mortar

Constant	Unit	Mortar
E_0	MPa	8030
ν_0	-	0.175
f_c	MPa	-7.39
A	MPa^{-2}	2500×10^{-5}
B	MPa^{-2}	100.0×10^{-5}
C	MPa^{-1}	-1.000×10^{-5}
D	MPa^{-1}	2.188×10^{-5}
F	-	6.000

a) b)

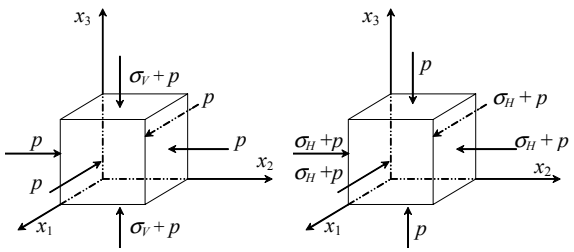

Fig. 1. Stress tensor components: a) tri-axial state of stress 1, b) tri-axial state of stress 2.

Table 2. Experimental and theoretical failure stress for mortar subjected to tri-axial state of stress 1

Specimen	Hydrostatic pressure p MPa	Failure stress σ_{33f} MPa	
		Experiment	Theory
ZC1	-1.05	-10.90	-11.48
ZD1	-1.05	-12.20	-11.48
ZC2	-2.05	-17.67	-15.65
ZD2	-2.05	-16.08	-15.65
ZC3	-3.05	-18.83	-19.60
ZD3	-3.05	-20.02	-19.60

Table 3. Experimental and theoretical failure stress for mortar subjected to tri-axial state of stress 2

Specimen	Hydrostatic pressure p MPa	Failure stress $\sigma_{11f} = \sigma_{22f}$ MPa	
		Experiment	Theory
ZA1	0	-7.19	-7.24
ZB1	-0.15	-9.40	-9.10
ZA2	-1.95	-15.89	-20.61
ZB2	-1.95	-16.83	-20.61
ZA3	-3.62	-23.55	-28.82
ZB3	-3.62	-24.87	-28.82

specimens). The configurations of the stress components in both tri-axial states of stress are shown in Fig. 1. The further details on equipment used and on experimental procedure adopted can be found in [5]. The objective of the test performed under uni-axial compression was to determine the initial Young modulus E_0 and Poisson ratio ν_0 as well as to measure the uni-axial compressive strength of the material f_c. The numerical values of these constant together with the other material parameters included in the theoretical model used in this note are shown in Table 1.
The loading paths for both tri-axial states of stress, shown in Fig. 1, were composed of two parts. The first stage of loading in both cases was the same and consisted in a monotonic increase of hydrostatic pressure up to prescribed value p. In the second stage of the tri-axial state of stress 1 (Fig.1a) the vertical normal stress σ_V was increased up to material failure. For tri-axial state of stress 2 shown in Fig. 1b the second stage of loading consist in simultaneous increase of two mutually perpendicular components σ_H up to material failure. The objective of the tests under tri-axial state of stress was to determine the respective stress-strain relations and to measure the failure load for each loading path. The numerical data concerning the prescribed values of the hydrostatic pressure p as well as maximum load sustained by the specimens are shown in Table 2 and 3.

BASIC EQUATIONS

Theoretical description of the experimental data presented here is based on own mathematical model developed and explained in [2,3]. The basic equation of this theoretical model is the stress strain relation

$$\varepsilon_{ij} = -\frac{\nu_0}{E_0}\delta_{ij}\sigma_{kk} + \frac{1+\nu_0}{E_0}\sigma_{ij} + C(\delta_{ij}D_{kl}\sigma_{kl} + D_{ij}\sigma_{kk}) + 2D(\sigma_{ik}D_{kj} + D_{ik}\sigma_{kj}) \tag{1}$$

which describes the anisotropic elastic response of the damaged material. Equation (1) contains the strain tensor ε_{ij}, the stress tensor σ_{ij}, the Kronecker delta δ_{ij}, the Young modulus E_0 and Poisson ratio ν_0 for an originally undamaged material, two constants C and D to be determined experimentally and the second order symmetric damage effect tensor D_{ij} responsible for the current state of internal structure of the material. Deterioration of the material structure due to applied load is described by the damage evolution equation expressed in the form of the tensor function

$$\Omega_{ij} = As_{kl}s_{kl}\left(1 + \frac{30\det\sigma_{pq}}{\left|\sigma_{ij}\sigma_{ik}\sigma_{kj}\right| + \left|\sigma_{ll}^3\right|}\right)^F \delta_{ij} + B\sqrt{\sigma_{kl}\sigma_{kl}}\left(1 + \frac{30\det\sigma_{pq}}{\left|\sigma_{ij}\sigma_{ik}\sigma_{kj}\right| + \left|\sigma_{ll}^3\right|}\right)^F \sigma_{ij} \tag{2}$$

where Ω_{ij} is a classical second order damage tensor, s_{kl} is the stress deviator and A, B, F are unknown material parameters to be determined experimentally. The equation

$$D_i = \frac{\Omega_i}{1-\Omega_i} \quad , \quad i = 1,2,3 \tag{3}$$

shows the relation between the principal components D_1, D_2 and D_3 of the damage effect tensor D_{ij} contained in Eqs. (1) and the principal values Ω_1, Ω_2 and Ω_3 of the damage tensor Ω_{ij} expressed by Eq. (2).
Equations (1), (2) and (3) and numerical data shown in Table 1 were used to construct the theoretical stress-strain curves and to determine the theoretically predicted maximum stress at material failure. The values of constants A, B, C, D and F seen in Table 1 and used in this analysis were determined experimentally according to the rules presented in [3]. The comparison of experimental and theoretical results obtained for the stresses at failure for various cases of tri-axial loading is shown in Table 2 and 3.

CONCLUSIONS

The study presented in this note makes it possible to conclude that theoretical stress-strain curves for tri-axial loading obtained from the relevant equations presented here show satisfactory agreement with experimental data determined for mortar subjected to various combinations of tri-axial compressions. Increasing compressive strength detected experimentally for specimens of mortar subjected to simultaneously applied hydrostatic pressure and uni-axial or bi-axial compression can also be explained theoretically within the mathematical model proposed.

References

[1] Halm D., Dragon A.: An Anisotropic Model of Damage and Frictional Sliding for Brittle Materials. *Eur. J. Mech. A/Solids* **17**: 439-460, 1998.

[2] Litewka A., Bogucka J., Debinski J.: Deformation Induced Anisotropy of Concrete. *Arch. Civil Eng.* **42**: 425-445, 1996.

[3] Litewka A., Debinski J.: Load-Induced Oriented Damage and Anisotropy of Rock-Like Materials. *Int. J. Plast*. **19**: 2171-2191, 2003.

[4] Murakami S, Kamiya K.: Constitutive and Damage Evolution Equations of Elastic-Brittle Materials Based on Irreversible Thermodynamics. *Int. J. Mech. Sci.* **39**: 473-486, 1977.

[5] Szojda L.: Analysis of Interaction of Masonry Structures and Deformable Foundation. *PhD Thesis*, Silesian University of Technology, Gliwice, 2001, (in Polish).